*Available online at*www.scholarsresearchlibrary.com

Scholars Research Library

Archives of Applied Science Research, 2015, 7 (5):118-128
(http://scholarsresearchlibrary.com/archive.html)

ISSN 0975-508X
CODEN (USA) AASRC9

Growth, structural, optical, thermal and photo conductivity studies of Potassium Hepta Fluoro Antimonate crystals

C. Besky Job

Department of Physics, Scott Christian College, Nagercoil, Tamil Nadu, India

---

ABSTRACT

Potassium Hepta Fluoro Antimonate crystals (KSb_2F_7) have been successfully grown by slow evaporation technique. Powder X-ray diffraction method has been used for structural identification. KSb_2F_7 crystallizes in the monoclinic system with the space group $P2_1/c$. The crystals having wide transmission spectra lying between 280 and 1100 nm. The optical characterization shows that the band gap energy of the crystal is 4.54 eV. The average refractive index in the visible region is 2.91.The peak value of optical conductivity is $4.07\times10^{10}S^{-1}$ in the UV region. The optical constants have been calculated and illustrated graphically. Thermal stability has been investigated by TGA/DTA and the melting point of the grown crystal has been found out as 252.4^0C. The photo conductivity study confirms the negative photo conductivity nature of the title compound.

Key words: Crystal growth, optical studies, band gap, refractive index, photo conductivity.

INTRODUCTION

In the context of unarguable interest on complex fluorides of trivalent antimony are characterized by the presence of an unshared pair of $5S^2$ electrons in a trivalent antimony atom [1]. The prominent Antimony Fluoride compounds (AFC) are $MSbF_4$, M_2SbF_5, MSb_2F_7, MSb_3F_{10}, MSb_4F_{13}, $M_2Sb_3F_{11}$ and $M_3Sb_4F_{15}$ (where M = Na, K, NH_4, Tl, Cs, Rb) [2]. The structure [3], superionic conduction [4,5], biocidal activity in marine bacteria [6] and TGA [7,8] studies of Potassium Hepta Fluoro Antimonate crystals (KSb_2F_7) had been already reported by the researchers for the last four decades.

Fluoride single crystals, owing to their unique properties such as large band gap has many advantages as optical materials [9]. Colquiriite type fluoride singe crystals are especially promising materials for UV laser and optical lithography applications [10]. Recently there is an increasing demand for the synthesis and growth of new electro-optic materials. Many complex fluorides of trivalent antimony possess unusual optical and other properties [11]. Scientists have made many attempts to find new ultraviolet (UV) and deep ultraviolet (DUV) nonlinear optical crystals. Compare with oxide crystals, fluoride crystals have larger band gap, therefore they are suitable for DUV harmonic generation. However, they have small second-harmonic coefficients, which is unfavorable for obtaining high power output at the harmonic frequencies [12]. Therefore we have made an attempt to find out optical constants include optical absorption coefficient (α), refractive index (n), extinction coefficient (k), optical conductivity (σ_{op}), dielectric constant and band gap (Eg) of KSb_2F_7 crystals. In this paper we report the structure, optical constants, mechanical and photo conductivity studies of KSb_2F_7 crystals.

MATERIALS AND METHODS

Crystal Growth

KSb_2F_7 crystal was synthesized by dissolving high purity AR grade Potassium fluoride (KF), Antimony tri oxide (Sb_2O_3) and Hydro fluoric acid (HF) in the molar ratio 1:1:6 in double distilled water and stirred well to form homogeneous solution. The chemical equation governing the reaction is,

$$KF+Sb_2O_3+6HF \rightarrow KSb_2F_7+3H_2O \quad (1)$$

The near saturated solution was transferred to a crystallizer and covered by a perforated polyethylene sheet for controlled evaporation at room temperature. After a growth period of two weeks, well developed and optically transparent KSb_2F_7 crystals have been harvested and was presented in Fig.1.

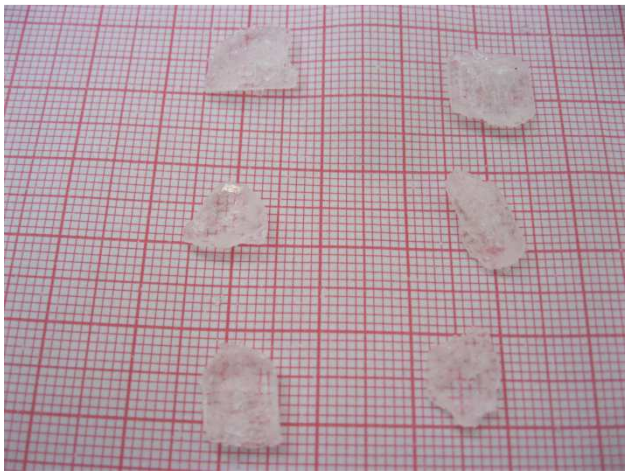

Fig. 1 Photograph of the grown KSb_2F_7 crystal

2.2. Materials Characterization

The grown KSb_2F_7 crystals have been analyzed by different characterization techniques. The powder X-ray diffraction study of the grown crystal has been carried out using Philips X'pert Pro X-ray Automatic diffractometer with CuKα radiation (λ=1.5418Å). ENRAF NONIUS CAD4 Automatic X-ray diffractometer with MoKα radiation (0.7107Å) was used to obtain the accurate cell parameters of the grown crystals. The UV-Vis spectrum for KSb_2F_7 crystal was recorded in the wavelength region of 100-1100 nm with the resolution of 1nm using Perkin Elmer Lambda 35 spectrophotometer. The photo conductivity studies of grown crystal has been carried out by connecting the sample in series with a dc power supply and a Keithley 480 Picco Ammeter. The applied filed was increased from 5 to 200 Vcm^{-1} , the corresponding dark current and photo current were recorded.

RESULTS AND DISCUSSION

3.1 XRD analysis

Figure 2 shows the standard and observed indexed XRD pattern of the grown KSb_2F_7 crystal. The observed XRD pattern has been compared with the JCPDS file no: 71-1945, confirms the presence of KSb_2F_7 crystal structure. Such a result has also been reported by S.H. Mastin et al [3]. From the single crystal X-ray diffraction studies it is found that the crystal exhibits monoclinic system with space group $P2_1/c$. The cell parameters were measured as a=10.51Å, b= 7.598Å, c=8.601Å and β=100.82°, Z=4. The calculated volume of the unit cell is 674.7$Å^3$. The lattice parameters are in good agreement with those values already reported, thus confirming the grown crystal [3].

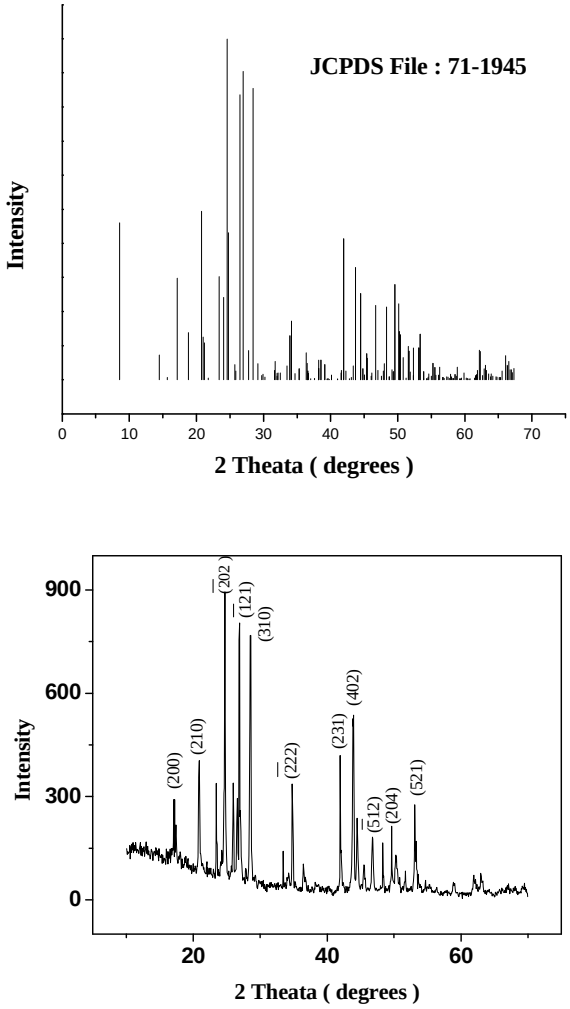

Fig. 2. Standard and Observed Indexed XRD pattern of KSb_2F_7 crystal

3.2 UV- Vis spectral analysis

The recorded optical transmission spectrum was shown in Fig 3. The crystal shows a good transmittance in the entire visible region and infrared region. The lower cut off wave length 280nm attest the usefulness of this material for opto electronics applications.

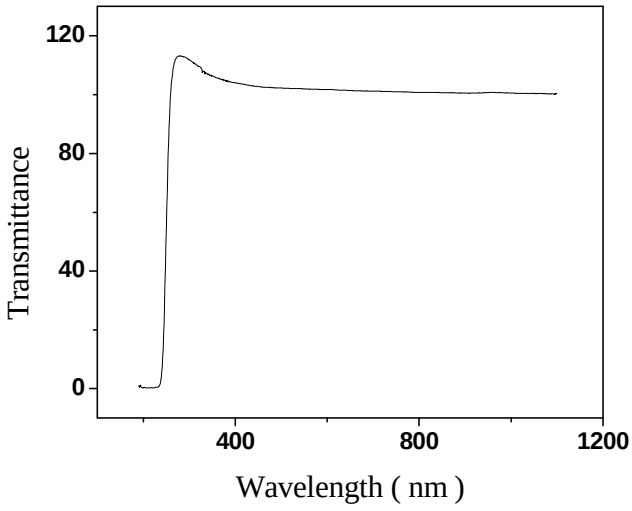

Fig. 3. Optical transmission spectra of KSb_2F_7 crystal

3.2.1 Determination of optical constants

Optical properties arise as a result of the interaction between photon energies and the structure or between the energy configuration of the materials [13]. When light is incident on the crystal, some of its energy is reflected, some is absorbed and rest is transmitted. The optical absorption of crystal varies with thickness and wavelength. The optical absorption coefficient (α) has been calculated from the transmittance using the relation [14],

$$\alpha = \frac{2.303 \log(1/T)}{d} \qquad (2)$$

Where T is the transmittance and d is the thickness of the crystal. Fig. 4 shows the dependence of optical absorption coefficient of the given crystal with the wavelength.

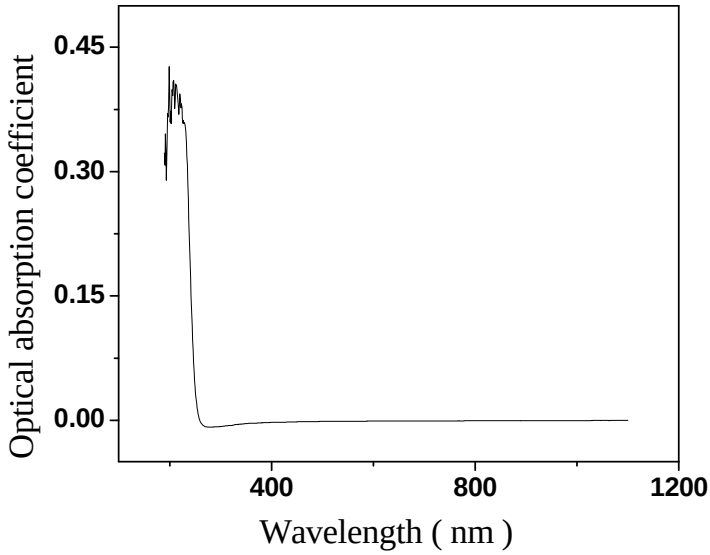

Fig. 4. Variation of optical absorption coefficient with wavelength for KSb_2F_7 crystal

The absorption coefficient obeys the Urbach's exponential relation [$\alpha=\alpha_0 \exp(h\nu/E_e)$], where E_e is the Urbach energy. E_e provides information about the extent of disorder. Absorption in this region is related to the transition between the extended states in one band and localized states in the exponential tail of the band. Hence disorder refers more towards that of electronic states within the materials compared to irregularity in atomic arrangement [15].

Photons of energy (hν) less than the optical energy gap of the crystals are not absorbed. Absorption starts at $h\nu=E_g$ and then increases rapidly. From the graph it is found that absorption increases exponentially below 274 nm.

According to Tauc [16], the relation between photon energy (hν) and absorption coefficient (α) is given by,

$$\alpha h\nu = A(h\nu - E_g)^n \qquad (3)$$

Where ν is the frequency, h is the Planck's constant, E_g is the optical band gap and n is a number which characterizes the optical processes : n= ½ for direct allowed transition, n=2 for indirect allowed transition, n=3/2 for forbidden direct allowed transition and n=3 for an indirect forbidden transition. The constant A is the slope of the Tauc edge called band tailing parameter that depends on the width of localized states in the band gap. When the straight portion of the plot of $(\alpha h\nu)^2$ against hν (Fig.5) is extrapolated to $\alpha^2=0$, the intercept gives the value of the optical band gap energy. The optical band gap value of KSb_2F_7 crystal has been found out as 4.54 eV.

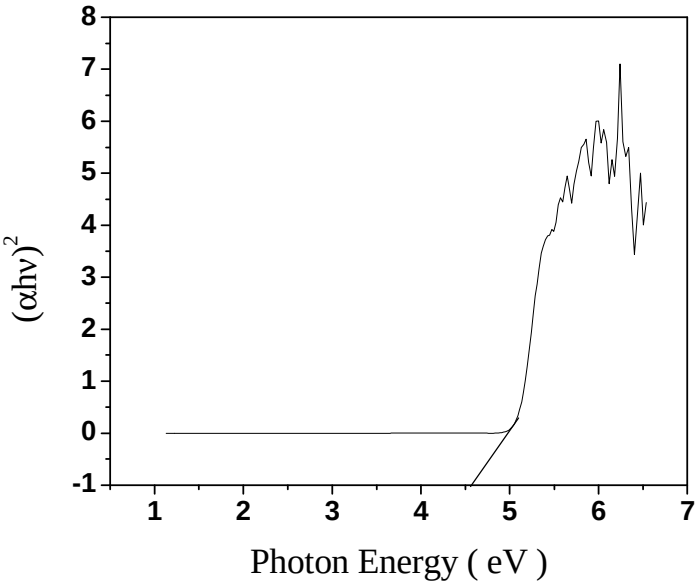

.

Fig. 5 Tauc's Plot for KSb_2F_7 crystal

The optical properties of a crystal can be evolved mainly from its optical transparency, band gap, extinction coefficient, the reflectance, refractive index, dielectric constant and optical conductivity. The optical properties of the crystals are governed by the interaction between the crystal and the electric and magnetic fields of the electro magnetic wave.

Extinction coefficient also called absorption index is a measure of the fraction of light loss due to scattering and absorption per unit distance in a participating medium [17]. In electromagnetic terms, the extinction coefficient can be explained as the decay or damping of the amplitude of the incident electric and magnetic fields. The extinction coefficient can be calculated using the relation,

$$k=\lambda\alpha/4\Pi \qquad (4)$$

Where λ is the wavelength, α is the optical absorption coefficient. The plot of Extinction coefficient versus wavelength is shown in Fig. 6.

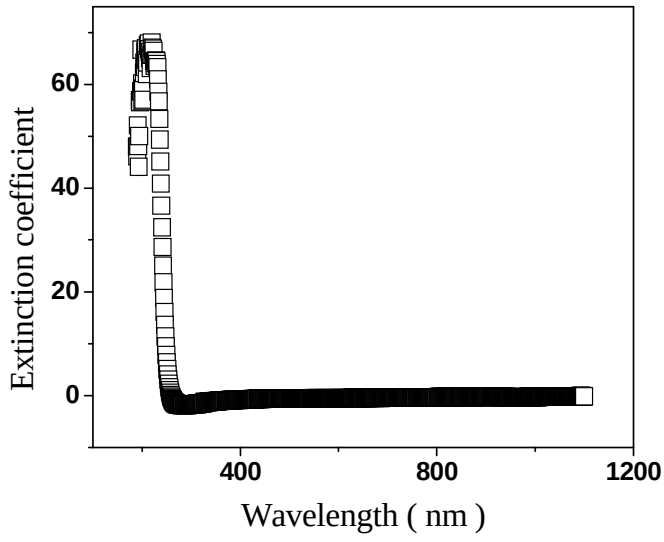

Fig. 6. Variation of Extinction coefficient as a function of wavelength for KSb_2F_7 crystal

The extinction coefficient has been found to decrease with the increase of wavelength under investigation. The average value of extinction coefficient in the visible region is 0.816. In the uv region its value increases up to 60 due to the increase in absorption. The decrease in the extinction coefficient with an increase in wavelength in the uv region shows that the fraction of light lost due to scattering and absorbance decreases.

The reflectance gives the ratio of the energy of reflected to incident light from a crystal. The reflectance (R) in terms of the absorption coefficient can be calculated using the relation[18],

$$R= \frac{1\pm\sqrt{(1-\exp(-\alpha t)+\exp(\alpha t)}}{1+\exp(-\alpha t)} \quad (5)$$

Where α is the optical absorption coefficient, t is the thickness of the crystal. Reflectance as a function of wavelength is graphically illustrated in Fig.7.

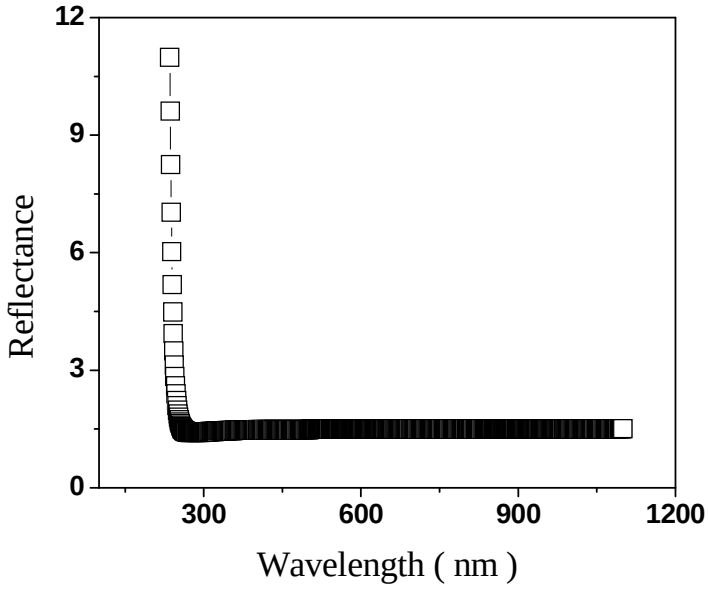

Fig. 7. Variation of Reflectance with wavelength for KSb_2F_7 crystal

The peak value of reflectance (11.03) occurs in the UV region at 240 nm. Refractive index of a substance (n) is a measure of the speed of light in that substance. The refractive index is a very important parameter related to the microscopic atomic interactions. If the crystal is consider as the collection of electric charges, the refractive index may be related to the density and the local polarizability of these entities [19]. Refractive index (n) has been calculated by using the relation [20],

$$n = \frac{-(R+1) \pm \sqrt{-3R^2 + 10R - 3}}{2(R-1)} \quad (6)$$

Where n- refractive index, R- Reflectance

The plot of wavelength versus refractive index for the grown crystal is shown in Fig.8.

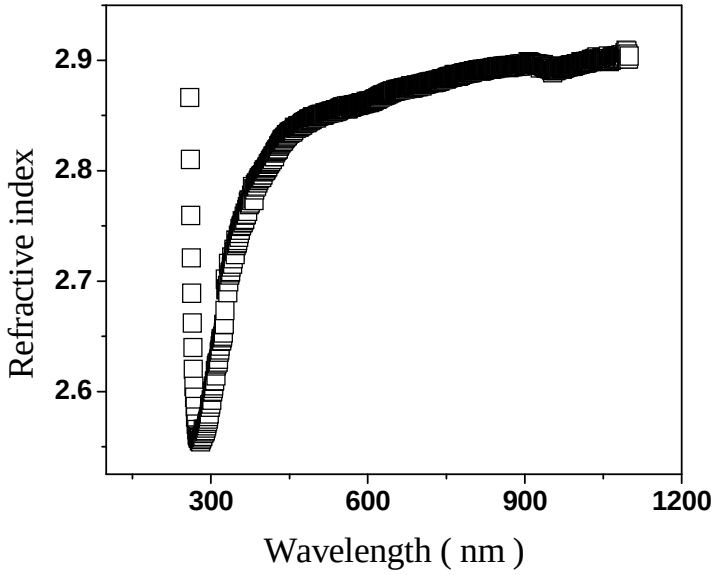

Fig. 8. Variation of refractive index with wavelength for KSb_2F_7 crystal

The average value of refractive index in the visible region is 2.91. This means that electromagnetic radiation is 2.91 times slower in crystals than in free space.

The complex dielectric constant is a fundamental intrinsic property of the material. The knowledge of the real and imaginary parts of the dielectric constant provides information about the loss factor which is the ratio of the imaginary part to the real part of the dielectric constant. The real dielectric constant (ε_r) is related to refractive index (n) and extinction coefficient (k) through the expression [21,22],

$$\varepsilon_r=n^2-k^2 \quad (7)$$

Imaginary dielectric constant

$$\varepsilon_i=2nk \quad (8)$$

The plot of real and imaginary dielectric constant with wave length is shown in Fig.9 and 10 respectively.

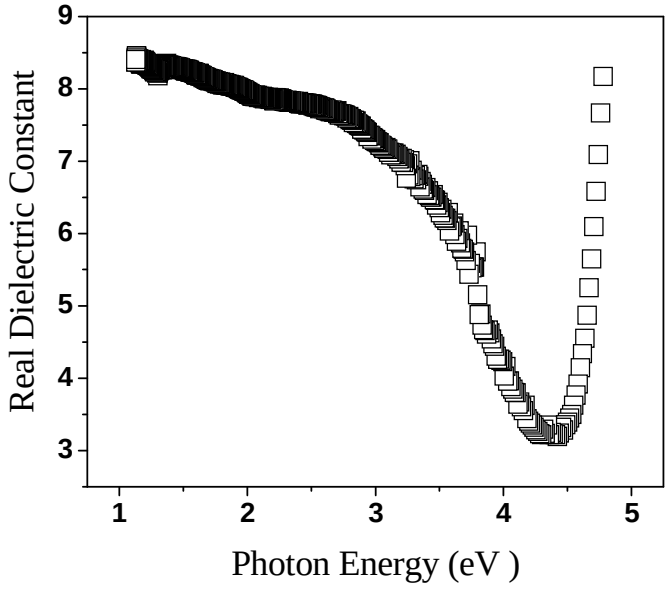

Fig. 9. Variation of Real dielectric constant with photon energy for KSb_2F_7 crystal

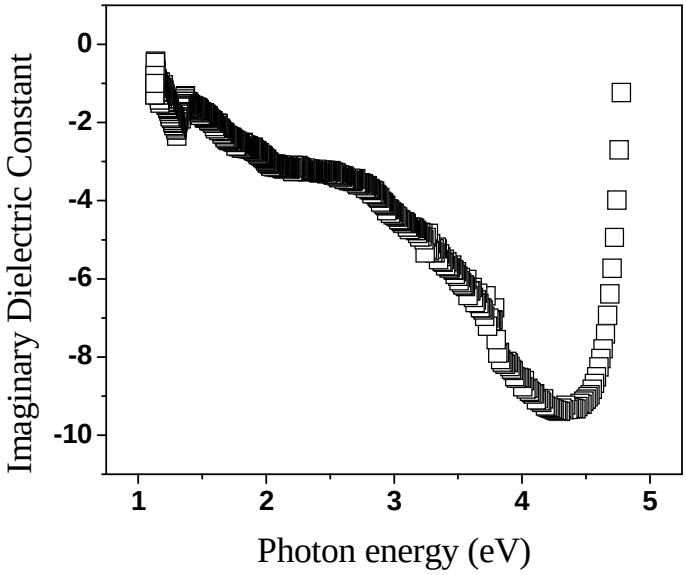

Fig. 10. Variation of Imaginary dielectric constant with photon energy for KSb_2F_7 crystal

The real dielectric constant ranged from 3.12 to 8.32. The imaginary dielectric constant ranged from1.18 to -9.48. Both real and imaginary dielectric constant decreases sharply with increase in photon energy and reaches the minimum value at 4.407 eV and again increases in the infrared region.

The real part of the dielectric constant is associated with the term that shows how much it will slow down the speed of light in the material and imaginary part shows how a dielectric absorbs energy from an electric field due to dipole motion [23].

The optical response of a material is studied in terms of the optical conductivity. It has dimensions of frequency which are valid only in a Gaussian system of units. The optical conductivity (σ_{op}) has been determined from the relation [24,25],

$$\sigma_{op} = \frac{\sigma n c}{4\pi} \qquad (9)$$

Where c is the velocity of light, α is the optical absorption coefficient and n is the refractive index. The variation of optical conductivity with wavelength is shown in Fig. 11.

Optical conductivity has a peak value of 4.07×10^{10} S^{-1} in the UV region. But the optical conductivity has very low values in the visible region. The sudden increase in optical conductivity in the UV region can be attributed to the increase in absorption coefficient.

3.3 Thermal studies

TGA/DTA curves of KSb_2F_7 crystal are shown in the Fig. 12 and 13 respectively. It is clear from the TGA curve that the material remains stable up to a temperature of about 250^0C. However, the weight loss of 3.732% in the low temperature region (50-130^0C) is assigned to the loss of water molecules. The endothermic peak at 252.4^0C is due to the melting point. The sharp endothermic peak shows the good crystalline perfection of the sample. When the temperature is increased above the melting point, there is a gradual and significant weight loss (35.8%) occurs at about 250-530^0C is due to the release of fluorine ions from the lattice of the crystal. Corresponding to a sub stage (530-960^0C), a weight loss of 26.85% is accompanied with the release of antimony trioxide from the crystal. A strong endothermic peak occurs in DTA at about 928.1^0C may be due to the second phase transition.

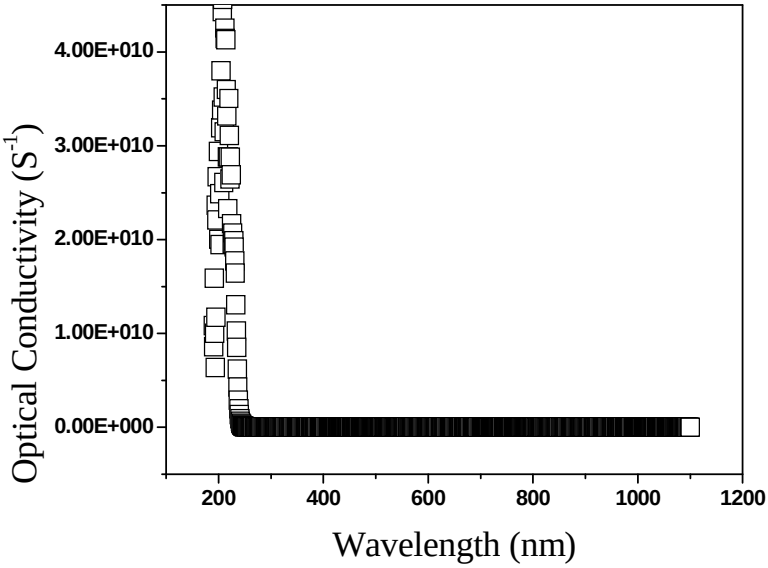

Fig. 11. Variation of Optical conductivity with wavelength for KSb_2F_7 crystal

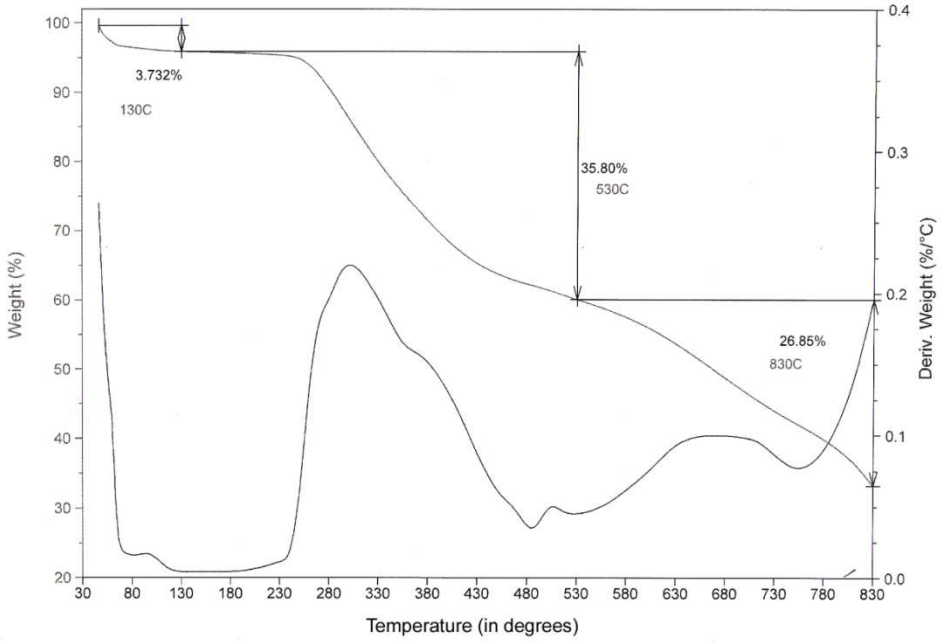

Fig. 12 TGA spectrum of KSb_2F_7 crystal

3.4 Photo conductivity studies

Field dependence of dark and photo current for KSb_2F_7 crystal was displayed in Fig. 14. It is observed from the plot that the dark current is greater than photo current, thus suggesting that KSb_2F_7 crystal exhibits negative photo conductivity [26]. This phenomenon was explained on the basis of stockman model. According to this model, negative photo conductivity is based on the two energy levels in which one is placed between the Fermi level and the conduction band while the other is located close to the valence band. The second state has high capture cross sections for electrons and holes. Also this state can capture electrons from the conduction band and holes from the valence band. Thus the net number of mobile charge carriers in the conduction band is reduced and giving raise to negative photo conductivity [27].

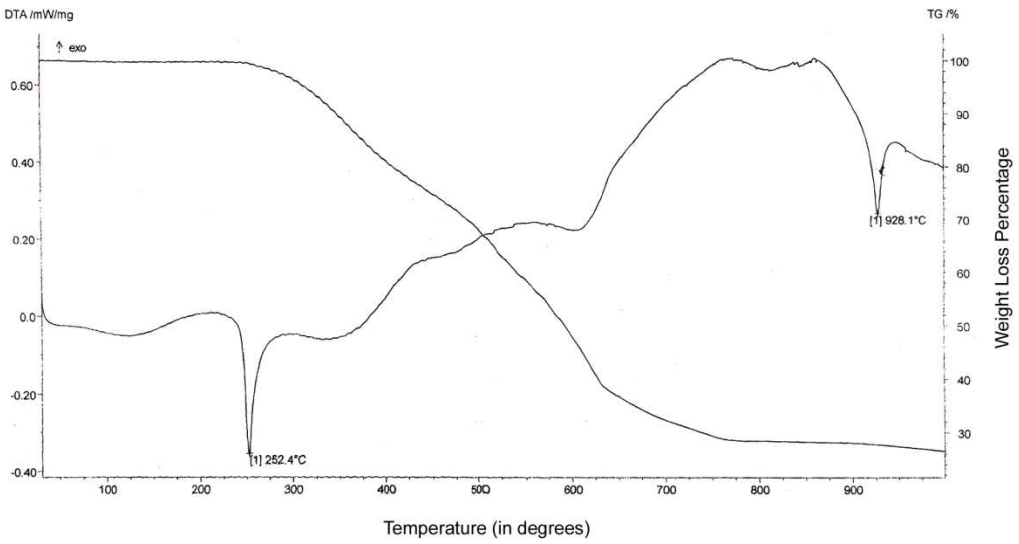

Fig. 13 DTA spectrum of KSb_2F_7 crystal

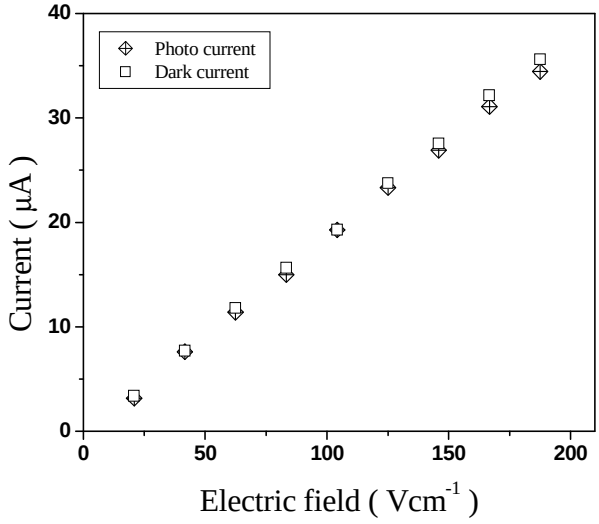

Fig.14 Field dependence of dark and photo current for KSb_2F_7 crystal

CONCLUSION

Good quality of KSb_2F_7 crystals were grown by slow evaporation method. Powder XRD analysis confirms the identity of the given crystals. KSb_2F_7 crystallizes in the monoclinic system with the space group $P2_1/c$. The grown crystal has good transmission window in the visible region between 280 nm and 1100 nm. The refractive index of the given crystal has average value of 2.91 within the visible region of the electro magnetic spectrum. The average extinction coefficient is 0.816. The highest value of optical conductivity in the uv region is 4.07×10^{10} S^{-1} .The highest values of real and imaginary parts of dielectric function were found to be 8.32 and 1.18 respectively. All these optical properties made this crystal to be a good candidate for opto electronics applications. KSb_2F_7 crystal shows negative photo conductivity.

REFERENCES

[1] V. N. Serezhikin, Yu. A. Buslaev, *Rus. J. Inorg. Chem.*, **1997,** 42, 1180.
[2] L. A. Zemnukhova, E. V. Kova leva, G. A. Fedorishcheva, V. V. Kon'shin, R. L. Davidovich, *Rus. J. Coord. Chem.*, **2004,** 30, 833.
[3] S. H. Mastin, R. R. Ryan, *Inorg. Chem.*, **1971,** 10, 1757.
[4] V. Ya. Kavun, N. F. Uvarov, A. B. Slobodyuk, O. V. Brovkina, L. A. Zemnukhova, V. I. Sergienko, *Rus. J. Electro Chem.*, **2005,** 41, 488.

[5] M. P. Borzenkova, F. V. Kalinchenko, A. V. Novo selova, A. K. Ivanov shits, N. I. Sorokin, *Rus. J. Inorg. Chem.*, **1984,** 29, 703.
[6] E. V. Kovaleva, L. A. Zemnukhova, V. H. Nikitin, M. D. Kovyakova, N. V. Speshneva, *Rus. J. App. Chem.*, **2002,** 75, 954.
[7] E. V. Kovaleva, L. A. Zemnukhova, N. Sh. Lebedeva, G. A. Fedorish cheva, *Rus. J. Coord. Chem*., **2005,** 31, 156 .
[8] R. L. Davidovich, L. A. Zemnukhova, *Rus. J. Coord. Chem*., **1975,** 1, 477.
[9] A. Cyrac Peter, M. Vimalan, P. Sagayaraj, J. Madavan, *Sch. Res . Lib*., **2010,** 2, 191 .
[10] A. Benaslah, K. Shimamura, K. Nakano, T. Fujita, T. Fukuda, *J. Crys. Growth*, **2001,** 23, 143.
[11] J. G. Bergman, D. S. Chemla, R. Four Cade, G. Mascherpa, *J. Solid State Commun*., **1978,** 3, 187.
[12] Yongzai Tong, X. Y. Meng, Z .Z. Wang, Chuangtian Chen, Ming-Hsien Lee, *J. App. Phys*., **2005,** 98, 033504.
[13] P. A. Cox, The Electronic Structure and Chemistry of Solids, Oxford University Press, Oxford, **1978**.
[14] J. I. Pankove, Optical Process in Semiconductors, Prentice Hall, Newyork, **1971**.
[15] Pankaj Sharma, S. C. Katyal, *Mat. Chem. and Phys.*, **2008,** 112, 892.
[16] J. Tauc, The Optical Properties of Solids, North-Holland, Amsterdam, **1970**.
[17] Nabeel A Bakr, A. M. Funde, V. S. Waman, M. M. Kamble, R. R. Hawaldar, D. P. Amalnerkar, *Pramana*, **2011**,76, 519.
[18] Jain John, P. Christuraj, K. Anitha, T. Bala Subramanian, *Mat. Chem. and Phy*., **2009**, 118, 284.
[19] R. Das, Prashant K. Sahu, *J. Optoelec. and Adv. Mat*., **2010,** 12, 1406.
[20] S. Suresh, A. Ramanand, P. Mani, Kaliyamurthy Anand, *J. Optoelect. and Biomedical Mat*., **2010,** 1, 129.
[21] A. Chalkwoski, Dielectric Physics, Elservier Scientific, Amsterdam, **1980**.
[22] P. A. Ilenikhena, *African Phy. Rev*., **2008,** 2, 68.
[23] R. Tintu, K. Saurav, K. Sulakshna, VPN Nampoori, P. Radakrishnan, Sheenu Thomas, *J. of Non oxide Glasses*, **2010,** 2, 167 .
[24] F. J. Blatt, Physics of Eletronic Conduction in Solids, McGraw Hill, New York, **1968**.
[25] I. M. Tsidilkovski, Band Structure of Semiconductors, Pergamon Press, Oxford, **1982**.
[26] R. H. Bube, Photoconductivity of Solids, Wiley, New York, **1981**
[27] Sagadevan Suresh, *The African Review of Physics*, **2013,** 0006, 8